remote sensing

MDPI

Article

Fusion of Ultrasonic and Spectral Sensor Data for Improving the Estimation of Biomass in Grasslands with Heterogeneous Sward Structure

Thomas Moeckel *, Hanieh Safari, Björn Reddersen, Thomas Fricke and Michael Wachendorf

Department of Grassland Science and Renewable Plant Resources, University of Kassel, Steinstr. 19, D-37213 Witzenhausen, Germany; safari.hanieh@gmail.com (H.S.); BReddersen@gmx.de (B.R.); thfricke@uni-kassel.de (T.F.); mwach@uni-kassel.de (M.W.)

* Correspondence: thmoeck@uni-kassel.de; Tel.: +49-5542-981337

Academic Editors: Lalit Kumar, Onisimo Mutanga, Lars T. Waser and Prasad S. Thenkabail

Received: 17 November 2016; Accepted: 17 January 2017; Published: 21 January 2017

Abstract: An accurate estimation of biomass is needed to understand the spatio-temporal changes of forage resources in pasture ecosystems and to support grazing management decisions. A timely evaluation of biomass is challenging, as it requires efficient means such as technical sensing methods to assess numerous data and create continuous maps. In order to calibrate ultrasonic and spectral sensors, a field experiment with heterogeneous pastures continuously stocked by cows at three grazing intensities was conducted. Sensor data fusion by combining ultrasonic sward height (USH) with narrow band normalized difference spectral index (NDSI) (R^2_{CV} = 0.52) or simulated WorldView2 (WV2) (R^2_{CV} = 0.48) satellite broad bands increased the prediction accuracy significantly, compared to the exclusive use of USH or spectral measurements. Some combinations were even better than the use of the full hyperspectral information (R^2_{CV} = 0.48). Spectral regions related to plant water content were found to be of particular importance (996–1225 nm). Fusion of ultrasonic and spectral sensors is a promising approach to assess biomass even in heterogeneous pastures. However, the suggested technique may have limited usefulness in the second half of the growing season, due to an increasing abundance of senesced material.

Keywords: pasture biomass; ground-based remote sensing; ultrasonic sensor; field spectrometry; sensor fusion; short grass

1. Introduction

To understand the spatio-temporal changes of forage resources in pasture ecosystems and to support grazing management decisions, an accurate estimation of biomass is needed [1–3]. However, a timely evaluation of biomass is a challenge, as it requires targeted and efficient means to assess numerous data for the creation of continuous maps. Though the traditional "clip-and-weigh" methods of measuring biomass are highly accurate, it is costly, destructive, labor-intensive and time-consuming to obtain biomass properties at a high sampling density. Alternatively, ground-based remote sensing techniques have been used as rapid and non-destructive methods to obtain and map the temporal and spatial variability of vegetation characteristics with high spatial resolution in agricultural and pastoral ecosystems [4–6]. Pastures are highly heterogeneous systems due to variations in sward structure, composition and phenology as well as continuous changes caused by different drivers such as environmental factors and grazing. Therefore, the application of sensors in complex grazing systems is difficult and there are some limitations for each specific sensor used for the prediction of sward characteristics [7,8]. To overcome these constraints, the combination of complementary sensor technologies has been suggested to utilize both the strengths and compensate the weaknesses of

individual technologies. Combined sensor systems can support multi-source information acquisition and may provide more accurate property estimates and eventually improved management [9]. Even though some studies have investigated such strategies in different farming fields [10,11], to date, these techniques have not been tested in pastures with complex sward diversity. Thus, an evaluation of sward specific calibration is essential before assessing data on a spatial scale.

Ultrasonic and reflectance sensors are two possible complementary technologies capable of providing comprehensive structural and functional characteristics of vegetation [4,10,12–15]. Sward height measured by ultrasonic distance sensing (referred to as ultrasonic sward height (USH)) has been examined as a possible estimator of biomass in forage vegetation canopies [5,16]. However, the main limitation of this technique is that signals are reflected predominantly from the upper canopy layers, regardless of sward density [4]. Moreover, sonic reflections can be affected by canopy architecture, such as lamina size, orientation, angle and surface roughness of the leaves [5,16,17].

Hyperspectral sensors have also raised considerable interest as a potential tool for prediction of biomass and forage quality in pastures. However, difficulties occur at advanced developmental stages of vegetation, as the ability of the reflectance sensor to detect canopy characteristics could be limited by the presence of a high fraction of senescent material in biomass [18,19] or soil background effects [18], atmospheric conditions [20], grazing impact [21] and heterogeneous canopy structures due to mixed species composition and a wide range of phenological stages [1,22,23]. Remarkably, most studies utilizing remotely sensed data for the estimation of grassland and rangeland biomass were conducted in tropical savannas, since these ecosystems account for 30% of the primary production of all terrestrial vegetation. In contrast, comparable studies on grasslands in temperate climates are rare [24].

The limitations of ultrasonic and hyperspectral reflectance sensors in heterogeneous pastures may be compensated by a combined use of measurement data from both sensors, as shown by [4] for less variable legume/grass-mixtures. Thus, the main objective of the present study was to analyze the potential of ultrasonic and hyperspectral sensor data fusion in pastures with high structural sward diversity to predict biomass, which is a prerequisite for future mapping of spatially heterogeneous grassland.

2. Materials and Methods

2.1. Study Area and Site Characteristics

For data acquisition, a long-term pasture experiment was chosen at the experimental farm Relliehausen of the University of Goettingen (51°46′55″N, 9°42′13″E, 180–230 m above mean sea level; soil type: pelosol-brown earth; soil pH: 6.3; mean annual precipitation: 879 mm; mean annual daily temperature: 8.2 °C). The plant association was a moderately species-rich *Lolio-Cynosuretum* [25]. The pastures exhibited pronounced heterogeneity in sward structure, with short and tall patches and various sward height classes [26,27]. Three levels of grazing intensity were allocated to adjacent pasture paddocks of 1 ha size, which were continuously stocked by cows from the beginning of May to mid-September. Grazing intensities were: (a) moderate stocking, average of 3.4 standard livestock units (SLU, i.e., 500 kg live weight) ha^{-1}; (b) lenient stocking, average 1.8 SLU ha^{-1}; and (c) very lenient stocking, average 1.3 SLU ha^{-1} [25]. To ensure extensive sward variation for data assessment, one representative study plot of 30 × 50 m size was selected within each of the three paddocks using a grazed/ungrazed-classified aerial image to obtain comparable surface proportions.

2.2. Field Measurements

Field measurements were conducted at four sampling dates (designated from now on as Date 1 to Date 4) in 2013: (Date 1) 25 April to 2 May (before grazing), (Date 2) 3 to 5 June, (Date 3) 21 to 23 August and (Date 4) 30 September to 2 October (after final grazing) within each study plot. In each campaign, 18 reference sample plots (each 0.25 m^2) were chosen within each of the 3 study plots,

adding up to a total of 54 samples per date which represented the existing range of available biomass levels and sward structures. To verify a representative biomass range, a stratified random sampling was performed. In each study plot, three levels of sward height (low, medium, and high) were sampled randomly to compile all date-specific biomass levels in the data set. A Trimble GeoXH GPS device (Trimble Navigation Ltd., Sunnyvale, California, USA) with DGPS correction from AXIO-net (Hannover, Germany, PED-RTK ±20 mm) was used to avoid repeated sampling at the same location during the growing season.

2.2.1. Ground-Based Remote Sensing Measurements

Sensor measurements took place prior to reference data assessment. Hyperspectral data was measured using a hand-held portable spectro-radiometer (Portable HandySpec Field VIS/NIR, tec5, Germany) in a spectral range of 305–1700 nm. Spectral readings were recorded in 1 nm intervals. Measurements were made from a height of about 1 m above and perpendicular to the soil surface between 10:00 a.m. and 2:00 p.m. (local time) in clear sunshine. The sensor had a field of view of 25°. Spectral calibrations were performed at least after every six measurements using a greystandard (Zenith® Diffuse Reflectance Standard 25%). Ultrasonic sward height (USH) measurements took place subsequent to hyperspectral measurements using an ultrasonic distance sensor of type UC 2000-30GM-IUR2-V15 (Pepperl and Fuchs, Mannheim, Germany). The sensor specific sensing range was from 80 to 2000 mm within a sound cone formed by an opening angle of about 25° [28]. Ultrasonic sward height (mm) was calculated by subtracting the ultrasonic distance measurement value in mm from the sensor mount height using Equation (1).

$$\text{USH (mm)} = \text{Mount height (mm)} - \text{Ultrasonic distance (mm)} \quad (1)$$

At each sampling plot, five measurements were recorded with the ultrasonic sensors placed at five positions on a frame at a height of about 1 m. Further details of the USH device and methodology can be found in Fricke et al. [5]. In addition to sensor measurements, plant composition of all sampling plots was assessed according to the method of Klapp and Stählin [29] by visually estimating the abundance and dominance of all plant species.

2.2.2. Sampling of Reference Data

The biomass of each sampling plot was cut at ground surface level. Total fresh matter yield was measured and representative sub-samples were either directly dried in the oven for 48 h at 105 °C for the calculation of total dry matter yield or sorted into fractions of grasses, legumes, herbs, mosses and dead material and subsequently also dried at 105 °C for 48 h to determine the proportion of each functional group. These data were used as reference values (dependent variables) in regression analysis procedures.

2.3. Data Analysis

Prior to analysis, an insignificant number of outliers (maximum two were excluded), which appeared as extreme outliers in the box plot analysis [30], were excluded from the dataset due to incorrectly entered or measured data. Moreover, noisy parts of the hyperspectral data (305–360 nm, 1340–1500 nm and 1650–1700 nm) were eliminated, leaving 1126 spectral bands between 360 and 1650 nm. Datasets were combined using a common dataset (n = 214) comprising samples from all study plots (grazing intensities) and all dates, as well as subsets for each date representing a typical phenological status of plants during the vegetation period (n = 52−54). A modified partial least squares regression (MPLSR) was applied as a powerful and full-spectrum based method to analyze the original reflectance values using the WINISI III package (Infrasoft International, LLC. FOSS, State College, PA, version 1.63). To evaluate the potential of a 2-band vegetation index across the available hyperspectral range, the normalized difference spectral index (NDSI) [31] was applied over the range of all single

(n = 1126) wavebands using all possible combinations of two-band reflectance ratios based on the NDVI formula [32] according to Equation (2):

$$\mathrm{NDSI}\,(b1,\ b2) = b1 - b2/\ b1 + b2 \tag{2}$$

where b1 and b2 represent spectral bands of reflection signals with Wavelength b1 > Wavelength b2.

To test the performance of the multispectral approach used in satellites, hyperspectral data were re-combined into 8 broad wavebands according to WorldView-2 satellite images: coastal (400–450 nm), blue (450–510 nm), green (510–580 nm), yellow (585–625 nm), red (630–690 nm), red edge (705–745 nm), near infrared-1 (770–895 nm) and near infrared-2 (869–900 nm) (http://www.landinfo.com/WorldView2.htm).

Ordinary least squares regression analysis was performed using the statistical program R to examine the relationship between the dependent variables (fresh matter yield, dry matter yield and dead material proportion) and USH (Equation (3)), NDSI and satellite bands exclusively (Equations (4) and (5)) and as a combination of USH with variables calculated from hyperspectral data (Equations (6) and (7)) to compare their potential for sensor fusion. After having examined the data and verified that saturation effects could be excluded, it was assumed that squared variables would sufficiently represent possible non-linear effects. Regardless, due to the limited sample size of $n \leq 54$, squared satellite band variables were omitted from the regressions to reduce the risk of over-fitting.

Exclusive ultrasonic sward height

$$Y = \mathrm{USH} + \mathrm{USH}^2 \tag{3}$$

Exclusive vegetation index

$$Y = \mathrm{NDSI} + \mathrm{NDSI}^2 \tag{4}$$

Exclusive satellite bands

$$Y = X1 + X2 + \ldots + Xn \tag{5}$$

Combination of ultrasonic sward height and vegetation index

$$Y = \mathrm{USH} + \mathrm{NDSI} + \mathrm{USH} \times \mathrm{NDSI} + \mathrm{USH}^2 + \mathrm{USH}^2 \times \mathrm{NDSI} + \mathrm{NDSI}^2 + \mathrm{USH} \times \mathrm{NDSI}^2 + \mathrm{USH}^2 \times \mathrm{NDSI}^2 \tag{6}$$

Combination of ultrasonic sward height (USH) and satellite bands

$$Y = \mathrm{USH} + \mathrm{USH}^2 + X1 + X2 + \ldots + Xn + \mathrm{USH} \times X1 + \ldots + \mathrm{USH} \times Xn + \mathrm{USH} \times X1 + \ldots + \mathrm{USH}^2 \times Xn \tag{7}$$

where Y = fresh matter yield (FMY) ($g \cdot m^{-2}$), dry matter yield (DMY) ($g \cdot m^{-2}$) or dead material proportion (DMP) (% of DMY); USH = ultrasonic sward height (mm); NDSI = 2-band combination vegetation index derived from hyperspectral data based on original NDVI formula; and X = WorldView-2 satellite bands.

To determine the best NDSI wavebands in order to maximize R^2, wavelength selection was first conducted according to Equation (4) and (6) for each target parameter. Thus, all possible 2-band NDSI combinations, in all 633,375 indices, were individually used in linear regression models for each sensor combination. The best fit wavelengths for the full models were then used to develop regression models. According to the rules of hierarchy and marginality [33,34], non-significant effects were excluded from the models using a step-wise approach, but were retained if the same variable appeared as part of a significant interaction at α-level of 5%. In order to reduce the risk of over-fitting, all models were validated by a four-fold cross validation method [35]. The prediction accuracy was evaluated using two measures: (a) the cross-validated squared correlation coefficient (R^2_{CV}), which describes the linear relation between the measured dependent variables (i.e., FMY, DMY, and DMP) and the values predicted by the linear model; and (b) the cross-validated root mean square error ($RMSE_{CV}$), which describes the average deviation of the estimated values from the observed ones.

3. Results

3.1. Sward Characteristics

Biomass as FMY and DMY varied from 68.8 to 3207 g·m^{-2} and from 29.2 to 691.9 g·m^{-2} with an overall mean value of 823.9 g·m^{-2} and 276.4 g·m^{-2}, respectively, for all sampling dates (Table 1). The sampling date at the beginning of June (Date 2) exhibited the highest biomass (mean value of 1240 g·m^{-2} and 314.5 g·m^{-2} for FMY and DMY, respectively), whereas Date 4 showed the lowest biomass (mean value of 567.5 g·m^{-2} and 237.6 g·m^{-2} for FMY and DMY, respectively). USH ranged from 7 to 646 mm during the growing season and the lowest sward heights were found at Date 1 (mean value = 136 mm). A wide range of DMP (1.4% to 83.6% of DM; sd = 20.5%) was observed throughout the growing season. The highest variability of DMP was observed at more advanced developmental stages of swards (Date 3 and 4; sd = 18.8% and 17.7% of DMY, respectively) which also delivered the highest mean values of DMP (45.7% and 40% of DMY, respectively). The proportion of grass was always considerably higher than proportions of legumes and herbs. The proportion of moss was negligible (overall mean value 1.9%). In total, 48 species were identified in the sampling plots (Table A1). The most important species were *Dactylis glomerata* (Constancy, C = 89.7%) and *Lolium perenne* (C = 70.1%) among the grasses, *Trifolium repens* (C = 39.7%) and *Trifolium pratense* (C = 17.8%) among the legumes, and *Taraxacum officinale* (C = 57.5%) and *Galium mollugo* (C = 40.7%) among the herbs.

Table 1. Descriptive statistics of dry matter yield, fresh matter yield, ultrasonic sward height and proportion of mosses, grasses, legumes, herbs and dead materials for common and date-specific swards.

	N	Min	Max	Mean	Sd	Min	Max	Mean	Sd
		Dry matter yield (g·m^{-2})				Fresh matter yield (g·m^{-2})			
Common	214	29.2	691.9	276.4	145.5	68.8	3207.0	823.9	554.6
Date 1	54	51.9	612.1	248.8	130.0	140.0	1883.0	739.6	416.9
Date 2	54	31.9	691.9	314.5	180.2	107.2	3207.0	1240.0	785.6
Date 3	52	68.2	654.8	305.7	138.1	148.0	1822.0	745.4	337.0
Date 4	54	29.2	468.8	237.6	112.7	68.8	1325.0	567.5	281.7
		Ultrasonic sward height (mm)				Grass proportion (% of DM)			
Common	214	7	646	252	151	8.0	93.7	50.6	23.9
Date 1	54	7	438	136	99	12.9	81.1	44.9	16.8
Date 2	54	31	646	364	174	8.2	93.7	72.2	19.0
Date 3	52	105	615	268	119	8.8	92.9	41.9	24.8
Date 4	54	48	576	240	107	8.0	85.3	43.1	20.6
		Legume proportion (% of DM)				Moss proportion (% of DM)			
Common	214	0.0	39.6	2.9	6.8	0.0	27.5	1.9	4.4
Date 1	54	0.0	36.4	4.7	8.2	0.0	21.3	4.9	6.1
Date 2	54	0.0	39.6	4.1	9.0	0.0	14.7	0.7	2.4
Date 3	52	0.0	31.2	1.9	5.0	0.0	27.5	1.6	4.4
Date 4	54	0.0	7.1	0.6	1.6	0.0	5.8	0.3	0.9
		Herb proportion (% of DM)				Dead material proportion (% of DM)			
Common	214	0.0	63.7	13.1	12.9	1.4	83.6	31.6	20.5
Date 1	54	0.0	44.6	13.6	12.7	2.5	70.3	31.9	14.9
Date 2	54	0.0	63.7	13.9	15.0	1.4	37.6	9.2	6.4
Date 3	52	0.0	47.5	14.6	12.8	3.9	76.3	40.0	18.8
Date 4	54	0.0	42.1	10.3	10.8	10.5	83.6	45.7	17.7

3.2. Exclusive use of Ultrasonic Sward Height

Prediction accuracies for DMY and FMY varied significantly between sampling dates and were predominately low (Figures 1 and 2). Higher accuracies were achieved at Date 1 both for DMY and FMY (R^2_{CV} = 0.73 and 0.80 respectively) when sward heights were much lower than at later dates.

The lowest R^2 values were found at Dates 3 and 4 ($R^2_{CV} < 0.40$). DMP had very weak or no correlation with USH and, thus, data are not shown.

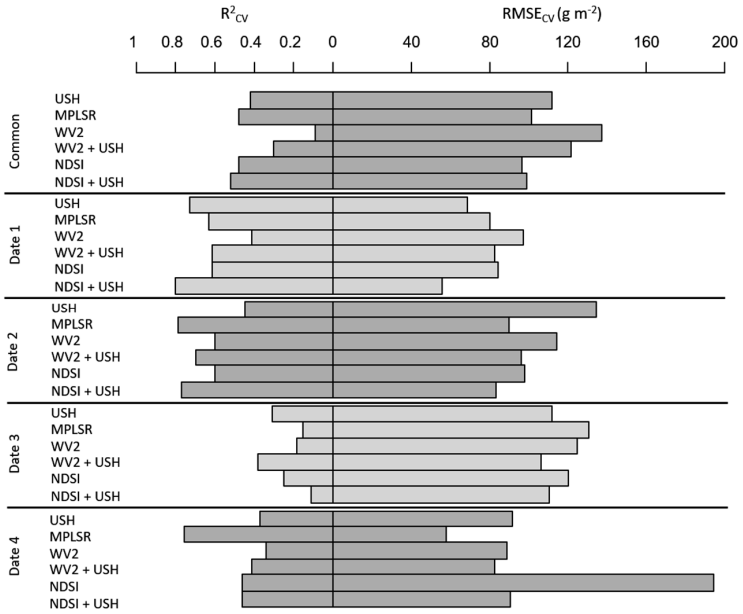

Figure 1. Cross-validation (CV) results for a range of sensor models used for prediction of fresh matter yield (FMY), including exclusive use of ultra-sonic sward height (USH), all hyperspectral wavebands using modified partial least squares regression (MPLSR), normalized difference spectral index (NDSI), and multispectral representation of WorldView-2 wavebands (WV2), as well as models formed from combinations of these sensors.

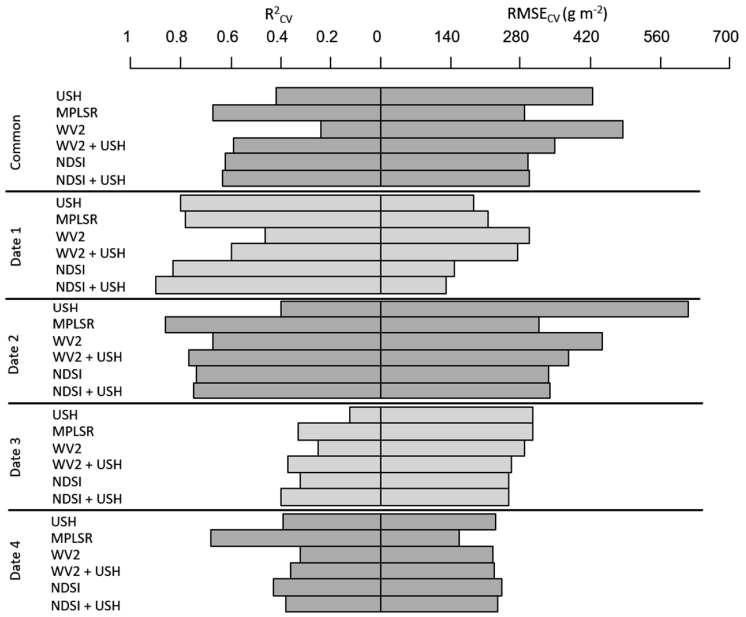

Figure 2. Cross-validation (CV) results for a range of sensor models used for prediction of dry matter yield (DMY), including exclusive use of ultra-sonic sward height (USH), all hyperspectral wavebands using modified partial least squares regression (MPLSR), normalized difference spectral index (NDSI), and multispectral representation of WorldView-2 wavebands (WV2), as well as models formed from combinations of these sensors.

3.3. Exclusive Use of Spectral Data

Maximum prediction accuracy based exclusively on NDSI was found mostly with bands between 1035 and 1139 nm, i.e., the ascending slope of the first water absorption band and the descending slope of the second water absorption band. The ascending slope of the second water absorption band (1188 to 1305 nm) was found to be the most important part of the spectrum for prediction of DMP (Table 2). Among models utilizing sensors exclusively, the MPLSR prediction accuracy was best both for DMY (R^2_{CV} of 0.48 for common and 0.15–0.79 for date-specific models) and FMY (0.67 and 0.33–0.86 respectively) (Figures 1 and 2). For DMP the MPLSR prediction was only best for the common model and date 1 (R^2_{CV} of 0.76 and 0.67), while for the other dates the NDSI showed the best results (R^2_{CV} between 0.43 and 0.68) (Figure 3). This regression approach integrates spectral information from the whole hyperspectral range and its usefulness for measuring grassland properties has been acknowledged by other studies [36–40]. The predictive power of WorldView2 (WV2) bands (R^2 0.13–0.55) was not satisfactory and never outperformed the NDSI or MPLSR approach.

Table 2. Wavelength position of best-fit band combination (b1, b2) for the normalized difference spectral index (NDSI) exclusively and in combination with ultrasonic sward height (USH) predicted target parameter.

	Common (n = 214)		**Date 1 (n = 54)**		**Date 2 (n = 54)**		**Date 3 (n = 52)**		**Date 4 (n = 54)**	
	b1	b2	b1	b2	b1	b2	b1	b2	b1	b2
Dry matter yield ($g \cdot m^{-2}$)										
NDSI	1035	1051	389	609	1097	1139	1122	1128	769	778
USH + NDSI	521	578	1215	1225	1024	1031	1116	1118	1622	1633
Fresh matter yield ($g \cdot m^{-2}$)										
NDSI	1117	1134	1040	1073	1080	1104	1122	1128	751	782
USH + NDSI	1077	1086	996	1005	536	564	1122	1135	1621	1633
Dead material proportion (% of dry matter yield)										
NDSI	1242	1305	1231	1285	1188	1202	1236	1281	1187	1206

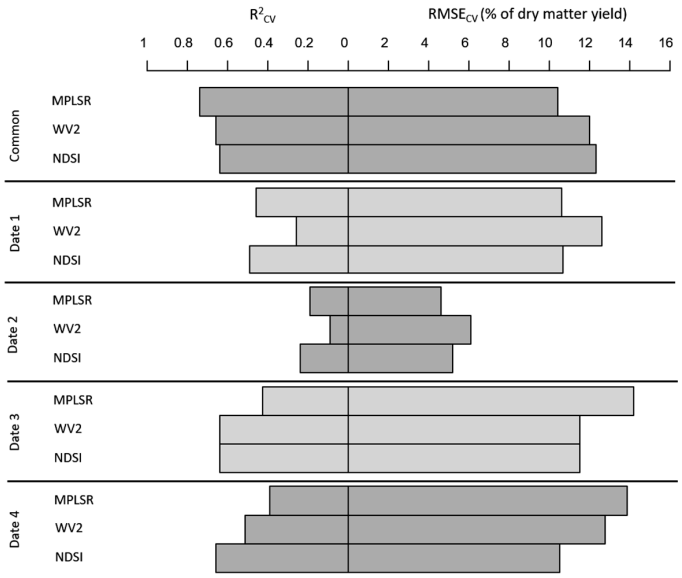

Figure 3. Cross-validation (CV) results for a range of sensor models used for prediction of dead material proportion (DMP), including exclusive use of all hyperspectral wavebands using modified partial least squares regression (MPLSR), normalized difference spectral index (NDSI), and multispectral representation of WorldView-2 wavebands (WV2) as explanatory variables.

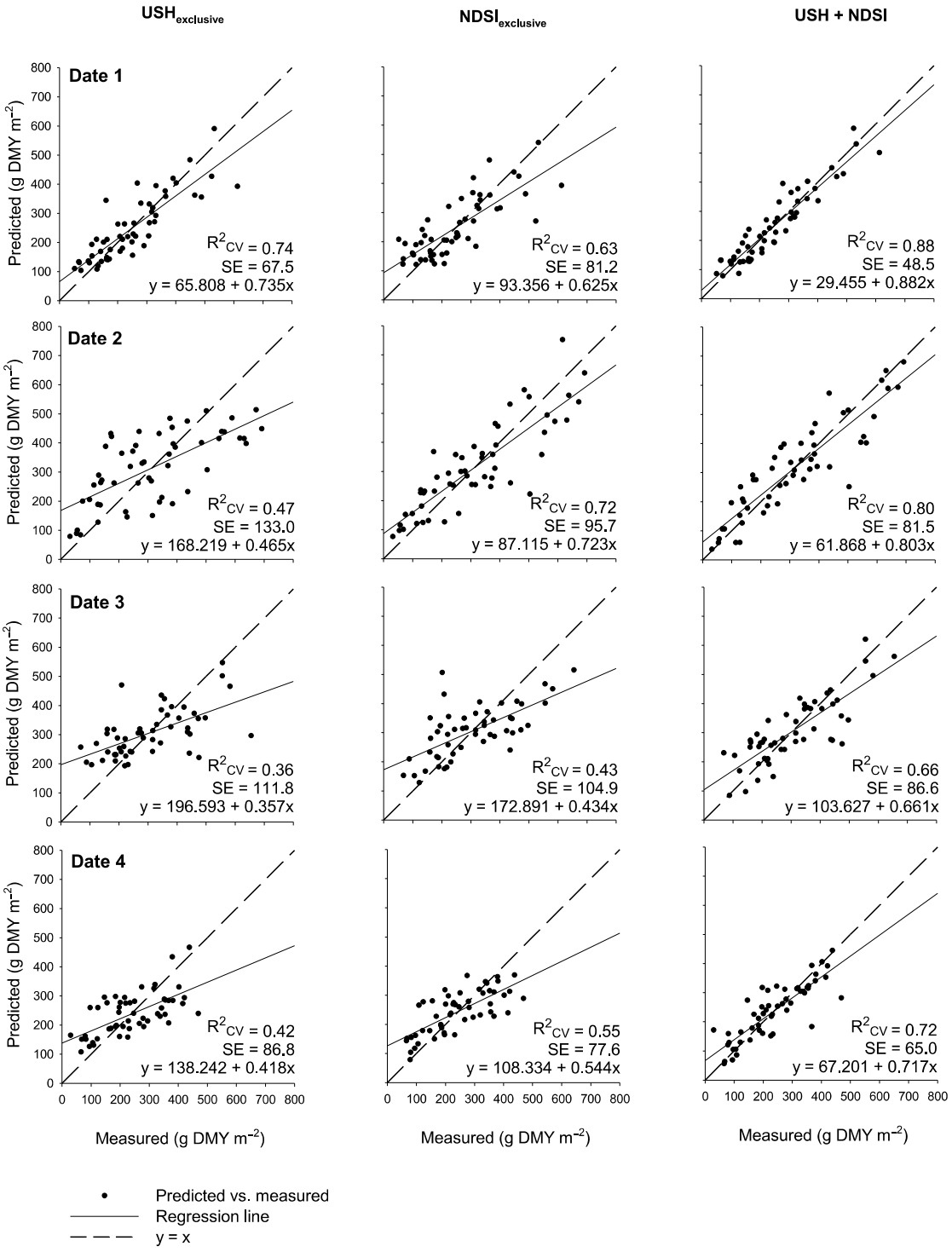

Figure 4. Plots of fit between measured and predicted dry matter yield (DMY) for exclusive use of ultrasonic sward height ($USH_{exclusive}$) and the best fit normalized difference spectral index ($NDSI_{exclusive}$) as well as a combination of USH and NDSI (USH + NDSI) applied in date-specific swards.

3.4. Sensor Data Fusion Using Combinations of USH and Spectral Variables

Combination of USH with the applied spectral variables increased R^2_{CV} -values for common swards from 0.42 (USH exclusively) to a maximum of 0.52 (NDSI combined with USH) for DMY and from 0.42 (USH exclusively) to a maximum of 0.63 (NDSI combined with USH) for FMY in common

swards (Figures 1 and 2). Irrespective of spectral sensor configuration, date-specific calibrations of yield parameters for Dates 1 and 2 performed better than for Dates 3 and 4. The combination of USH and NDSI consistently produced the best results, both in common and date-specific calibrations. Similar to the model findings with exclusive use of NDSI, the dominant bands of NDSI when in combination with USH were mostly located at water absorption bands, i.e., the ascending slop of the first absorption band (between 996 and 1086 nm) and the ascending slope of the second water absorption band (1215 to 1225 nm) as well as the green region in the visible spectrum (521 to 578 nm) (Table 2). Figure 4 shows example plots of fit for DMY prediction based on USH and NDSI and provides a comprehensive insight into the effects of sensor combination. It becomes clear that with exclusive use of sensors, calibration models led to an overestimation at low levels of DMY, whereas higher values were underestimated. An improvement of fit by combining sensors is obvious for all sampling dates (except Date 3), as demonstrated by higher R^2_{CV} -values and convergence of the regression line to the bisector. Yield predictions in heterogeneous pastures as presented in this study partly show a complex interaction between USH, NDSI and DMP (Figure 5). At higher levels of NDSI (here seen as a measure of, e.g., sward density), DMY and FMY basically follow a linear increase with USH gain (here seen as a measure for sward height), regardless of DMP. In contrast, at low levels of NDSI, DMY and FMY curves show differing trends. While DMY (Figure 5A) just shows a parallel shift to lower yield levels, FMY (Figure 5B) in swards with high DMP shows a saturated curve.

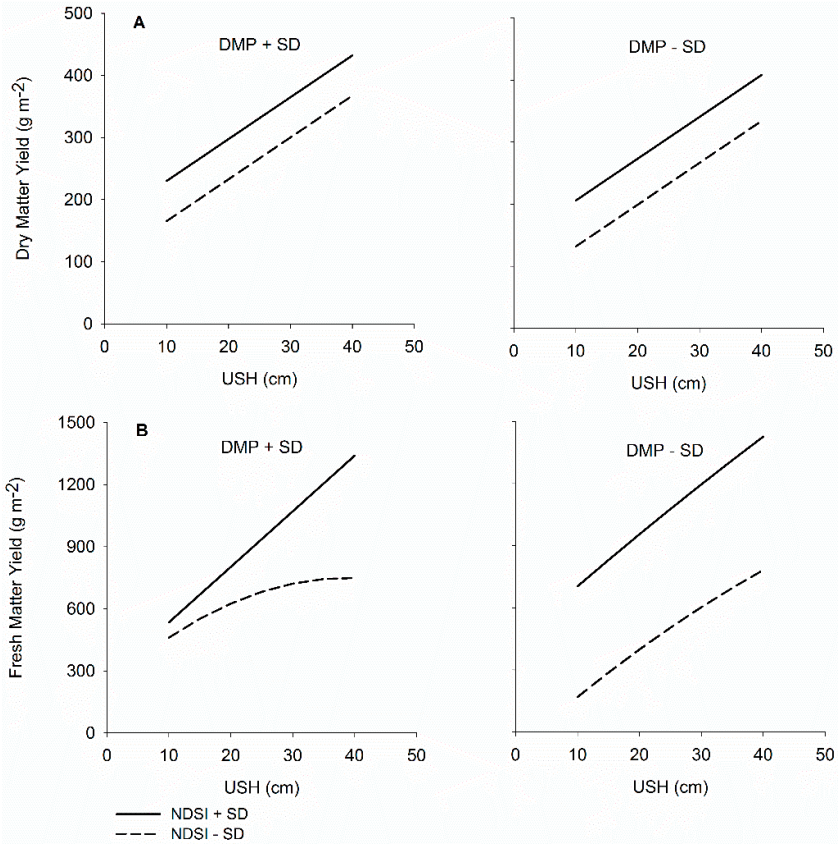

Figure 5. Predictions of dry matter yield (DMY) (**A**); and fresh matter yield (FMY) (**B**) in common swards based on ultrasonic sward height (USH) and the Normalized Difference Spectral Index (NDSI) as influenced by dead material proportion (DMP) in the range of ± standard deviation (SD). NDSI represents narrow-band reflection values selected in combination with USH for each parameter.

4. Discussion

4.1. Exclusive Use of USH

Sward height measured by ultrasonic sensors seems to become a poorer predictor of biomass with progression of the grazing season, as partly utilized patches were short in height but had a dense biomass. In addition, some species such as *Dactylis glomerata* and *Festuca rubra* frequently grow in dense tussocks and produce high biomass at low height, which results in an underestimation of biomass by USH (Figure 1). In some patches rejected by animals, very tall and mature species like *Cirsium arvense*, elongated stems of *Galium mollugo* or very tall and sparse individuals of *Phleum pratensis* at inflorescence stage occurred. Such sward structures may tend to be overestimated (Figure 1) and may have boosted USH measures although the amount of biomass was not particularly high. This effect was also observed by Fricke et al. [5], who further showed that the relationship between forage mass and USH could be influenced by weed proportion, as some weeds grow higher than the sown species. Beside the heterogeneity of canopy structure, variation in leaf angle among plant species and movements of swards during measurement due to wind may have further affected the reflection of ultrasonic signal [16,17]. In summary, exclusive use of USH measurements produced low prediction accuracies for yield parameters in heterogeneous pastures.

4.2. Exclusive Use of Spectral Data

Most spectral variables gave better prediction accuracies than exclusive use of USH measurements. This finding does not match that of Fricke et al. [4] and Adamchuk et al. [41] who reported that exclusive use of USH achieved better results than exclusive use of narrow or broad band spectral vegetation indices for prediction of biomass in more homogeneous grasslands. Contrary to yields, separation of the common dataset into date-specific subsets did not improve prediction accuracy for DMP (Figure 3). Yang and Guo [19] found that the relationship between dead material cover and spectral indices is a function of the amount of dead material, and they concluded that spectral indices could be used for estimating dead material cover which is greater than 50% in mixed grasslands. In this respect, the lower model accuracies for yield at later dates may be partly attributed to the higher amount of dead material at this time. The higher proportion of explained variance in DMP by spectral variables may reflect the impact of dead materials on the canopy reflectance at Date 3 (R^2_{CV} = 0.43–0.64) and, to a lesser degree, at Date 1 (R^2_{CV} = 0.26–0.49) and Date 4 (R^2_{CV} = 0.39–0.66). In contrast, DMP is much lower at Date 2, which corresponds to lower R^2_{CV} values for DMP prediction (0.09–0.24) (Figure 3), but allows higher accuracies for yield prediction, as low levels of DMP are inversely related to higher proportions of green plant material. This is consistent with findings by Chen et al. [42], who pointed out that spectral indicators usually collect data over green vegetation rather than mature and dry vegetation.

Dominant bands of NDSI were mostly located at water absorption bands. This dominance of water absorption bands can be explained by the strong relationship between biomass and canopy water content [43,44]. The importance of water absorption bands for estimating biomass is also confirmed by other investigations [4,45]. Numata et al. [22] found that water absorption features derived from hyperspectral sensors were better measures for estimating pasture biomass compared to spectral vegetation indices, such as Normalized Difference Vegetation Index and Normalized Difference Water Index. In summary, the yield of pastures with complex sward structures could barely be predicted using sensor measurements exclusively.

4.3. Sensor Fusion

Prediction accuracies of the combined measurements were high in the early stages of the grazing season. However, sward structures were so complex at later stages of the grazing season, that even sensor combinations did not produce satisfactory results. Considering the consequences of these limitations for the implementation of sensor data fusion in precision agriculture, it should be noted that the productivity of cool-season pastures is usually highest in the first half of the growing

season [46] when the best results with combined sensor data were obtained. Thus, sensor data fusion gains more importance in this particular part of the vegetation period, when efficient and timely estimates of available biomass is most relevant for grazing management decisions. Furthermore, major management measures (e.g., fertilization, evaluation of botanical sward composition) are also typically scheduled before summer, when pasture growth is frequently limited by water scarcity or progressively reduced day lengths.

The fusion of sonar and spectral variables always performed better in predicting yield parameters than the use of each sensor alone. However, the interactions between the two groups of variables with the measured vegetation parameter are complex, particularly for situations with high DMP. Pastures with high cover of dead material might consist of both compacted xeric material leading to higher yield levels at low sward height and sparse high growing mature shoots reaching higher sward layers without much contribution to yield. In contrast, at low DMP, NDSI seems to be more closely linked to pure sward density of green vegetation. The inter-relationship between selective grazing and species phenology creates a broad variation of sward structures posing an enormous challenge for any sensor applications.

Comparable to NDSI, WV2 bands also proved to be an effective spectral tool in combination with USH. This is of particular interest, as this finding points to the potential of the WordView-2 satellite system to provide large-scale images with an acceptable spatial resolution to assess larger pasture areas in farming practice. The relatively high prediction accuracy of WV2 bands, particularly in the major growth period during the first half of the year, opens up a perspective for the development of future management assistant tools. Continuous biomass monitoring based on advanced multispectral satellite images with high spatial resolution like WorldView and GeoEye can be used as support for management decisions such as the planning of grazing time and grazing intervals for cattle on pasture paddocks, site specific re-sowing or targeted cut of less-preferred sub-areas. However, further research is necessary to evaluate the availability of reliable images at a high repetition frequency and their combination with sward height data, as for instance, derived from radar satellites.

5. Conclusions

Mapping the spatio-temporal dynamics of pasture is a necessary prerequisite for making effective grassland management decisions and ensuring timely actions. In order to understand spatio-temporal dynamics, accurate measures of grassland characteristics, such as biomass, are needed, which should preferably be measured in a non-destructive manner. The present study revealed the potential of ultrasonic and hyperspectral sensor data as a non-destructive measurement method for the prediction of biomass in pastures characterized by a high structural diversity.

Our new approach of combining ultrasonic and hyperspectral sensor data improved the precision of biomass estimation when compared to the results gained by each single sensor. In particular, the combination of ultrasonic sensors with a selected subset of hyperspectral bands increased the prediction accuracy significantly. This finding may constitute a promising link to practical use because the identified bands are already implemented on satellite platforms.

However, the inter-relationship between selective grazing and species phenology poses an enormous challenge to sensor applications because it creates highly complex variation in sward structure. More advanced and complex sensor systems are needed to overcome such limitations and future studies should therefore aim at further systematically testing a variety of different sensor applications and their combinations. Purchasing a full range hyperspectral radiometer is still costly and is, therefore, hardly an economically feasible option for grassland managers. This poses another challenge for the practical applicability of the presented methods and should be considered in future studies. However, the increasing use of such sophisticated sensors leads to the assumption that prices will decrease in the future.

Acknowledgments: The authors would like to thank the section of Grassland Science, Georg-August-Universität Göttingen for the provision of experimental pastures and their kind cooperation. This project was supported by a

grant of the Research Training Group 1397 "Regulation of soil organic matter and nutrient turnover in organic agriculture" of the German Research Foundation (DFG). We thank the anonymous reviewers for their valuable comments on an earlier version of the manuscript.

Author Contributions: HS, TF, and BR conducted the fieldwork. All authors contributed equally to the data analysis and manuscript preparation.

Conflicts of Interest: The authors declare no conflicts of interest.

Appendix A

Table A1. List of pasture species identified in 214 sampling plots in 2013 with their minimum, maximum and mean values of dry matter contribution estimated according to the Klapp and Stählin method. Constancy (Const.) refers to the relative proportion of plots containing the respective species.

Species	Min	Max	Mean	Const. (%)	Species	Min	Max	Mean	Const. (%)
Grasses					**Herbs**				
Agrostis stolonifera	0.0	79.4	9.22	54.2	*Achillea millefolium*	0.0	85.0	0.92	5.1
Alopecurus pratensis	0.0	95.0	3.83	13.6	*Anthriscus sylvestris*	0.0	28.0	0.13	0.5
Arrhenatherum elatius	0.0	1.0	0.00	0.5	*Bellis perennis*	0.0	59.0	0.31	2.3
Bromus mollis	0.0	7.0	0.10	3.7	*Centaurea jacea*	0.0	1.0	0.00	0.5
Cynosurus cristatus	0.0	59.6	1.77	10.3	*Cerastium holosteoides*	0.0	4.0	0.23	19.6
Dactylis glomerata	0.0	94.0	25.68	89.7	*Cirsium arvense*	0.0	40.0	1.14	9.3
Deschampsia caespitosa	0.0	90.0	0.59	0.9	*Cirsium vulgare*	0.0	15.0	0.30	7.0
Elymus repens	0.0	80.0	5.82	36.9	*Convolvulus arvensis*	0.0	28.6	0.39	6.1
Festuca pratensis	0.0	85.0	0.71	5.6	*Crepis capillaris*	0.0	20.0	0.38	6.1
Festuca rubra	0.0	95.4	4.85	21.0	*Erophila verna*	0.0	4.0	0.04	4.7
Lolium perenne	0.0	88.6	15.64	70.1	*Epilobium spec.*	0.0	16.0	0.20	4.7
Phleum pratense	0.0	4.0	0.06	2.3	*Galium mollugo*	0.0	88.0	9.67	40.7
Poa annua	0.0	1.0	0.01	0.9	*Geranium dissectum*	0.0	13.0	0.20	13.6
Poa pratensis	0.0	45.0	2.32	27.6	*Geum urbanum*	0.0	30.0	0.19	3.3
Poa trivialis	0.0	16.0	1.28	25.2	*Hieracium pilosella*	0.0	0.2	0.00	0.5
					Lamium purpureum	0.0	38.0	0.21	2.3
Legumes					*Leontodon hispidus*	0.0	2.0	0.02	1.9
Medicago lupulina	0.0	5.0	0.03	0.9	*Plantago lanceolata*	0.0	35.0	0.56	10.7
Trifolium campestre	0.0	20.0	0.17	1.9	*Plantago major*	0.0	3.0	0.01	0.5
Trifolium dubium	0.0	25.0	0.18	3.7	*Taraxacum officinale*	0.0	83.0	5.89	57.5
Trifolium pratense	0.0	61.0	1.50	17.8	*Ranunculus acris*	0.0	10.0	0.20	6.5
Trifolium repens	0.0	49.6	2.49	39.7	*Ranunculus repens*	0.0	71.8	1.35	23.8
Vicia cracca	0.0	1.0	0.00	0.5	*Rosa spec.*	0.0	5.0	0.04	0.9
					Rumex acetosa	0.0	4.0	0.03	1.4
					Urtica dioica	0.0	84.0	1.09	2.8
					Veronica chamaedrys	0.0	4.0	0.03	1.9
					Veronica serpyllifolia	0.0	35.0	0.19	1.9

References

1. Cho, M.A.; Skidmore, A.; Corsi, F.; van Wieren, S.E.; Sobhan, I. Estimation of green grass/herb biomass from airborne hyperspectral imagery using spectral indices and partial least squares regression. *Int. J. Appl. Earth Obs. Geoinf.* **2007**, *9*, 414–424. [CrossRef]
2. Fava, F.; Colombo, R.; Bocchi, S.; Meroni, M.; Sitzia, M.; Fois, N.; Zucca, C. Identification of hyperspectral vegetation indices for Mediterranean pasture characterization. *Int. J. Appl. Earth Obs. Geoinf.* **2009**, *11*, 233–243. [CrossRef]
3. Xiaoping, W.; Ni, G.; Kai, Z.; Jing, W. Hyperspectral remote sensing estimation models of aboveground biomass in Gannan rangelands. *Proc. Environ. Sci.* **2011**, *10*, 697–702. [CrossRef]
4. Fricke, T.; Wachendorf, M. Combining ultrasonic sward height and spectral signatures to assess the biomass of legume-grass swards. *Comput. Electron. Agric.* **2013**, *99*, 236–247. [CrossRef]
5. Fricke, T.; Richter, F.; Wachendorf, M. Assessment of forage mass from grassland swards by height measurement using an ultrasonic sensor. *Comput. Electron. Agric.* **2011**, *79*, 142–152. [CrossRef]
6. Lee, H.-J.; Kawamura, K.; Watanabe, N.; Sakanoue, S.; Sakuno, Y.; Itano, S.; Nakagoshi, N. Estimating the spatial distribution of green herbage biomass and quality by geostatistical analysis with field hyperspectral measurements. *Grassl. Sci.* **2011**, *57*, 142–149. [CrossRef]
7. Schellberg, J.; Hill, M.J.; Gerhards, R.; Rothmund, M.; Braun, M. Precision agriculture on grassland: Applications, perspectives and constraints. *Eur. J. Agron.* **2008**, *29*, 59–71. [CrossRef]

8. Pullanagari, R.R.; Yule, I.J.; Hedley, M.J.; Tuohy, M.P.; Dynes, R.A.; King, W.M. Multi-spectral radiometry to estimate pasture quality components. *Precis. Agric.* **2012**, *13*, 442–456. [CrossRef]
9. Adamchuk, V.I.; Sudduth, K.A.; Lammers, P.S.; Rossel, R.A.V. *Sensor Fusion for Precision Agriculture*; In-Tech: Rijeka, Croatia, 2011.
10. Jones, C.L.; Maness, N.O.; Stone, M.L.; Jayasekara, R. Chlorophyll estimation using multispectral reflectance and height sensing. *Trans. ASABE* **2007**, *50*, 1867–1872. [CrossRef]
11. Mazzetto, F.; Calcante, A.; Mena, A.; Vercesi, A. Integration of optical and analogue sensors for monitoring canopy health and vigour in precision viticulture. *Precis. Agric.* **2010**, *11*, 636–649. [CrossRef]
12. Scotford, I.M.; Miller, P. Combination of spectral reflectance and ultrasonic sensing to monitor the growth of winter wheat. *Biosyst. Eng.* **2004**, *87*, 27–38. [CrossRef]
13. Scotford, I.; Miller, P. Estimating tiller density and leaf area index of winter wheat using spectral reflectance and ultrasonic sensing techniques. *Biosyst. Eng.* **2004**, *89*, 395–408. [CrossRef]
14. Farooque, A.A.; Chang, Y.K.; Zaman, Q.U.; Groulx, D.; Schumann, A.W.; Esau, T.J. Performance evaluation of multiple ground based sensors mounted on a commercial wild blueberry harvester to sense plant height, fruit yield and topographic features in real-time. *Comput. Electron. Agric.* **2013**, *91*, 135–144. [CrossRef]
15. Sui, R.; Thomasson, J.A. Ground-Based Sensing System for Cotton Nitrogen Status Determination. *Trans. ASABE* **2006**, *49*, 1983–1991. [CrossRef]
16. Hutchings, N.J.; Phillips, A.H.; Dobson, R.C. An ultrasonic rangefinder for measuring the undisturbed surface height of continuously grazed grass swards. *Grass Forage Sci.* **1990**, *45*, 119–127. [CrossRef]
17. Hutchings, N.J. Factors affecting sonic sward stick measurements: the effect of different leaf characteristics and the area of sward sampled. *Grass Forage Sci.* **1992**, *47*, 153–160. [CrossRef]
18. Boschetti, M.; Bocchi, S.; Brivio, P.A. Assessment of pasture production in the Italian Alps using spectrometric and remote sensing information. *Agric. Ecosyst. Environ.* **2007**, *118*, 267–272. [CrossRef]
19. Yang, X.; Guo, X. Quantifying Responses of spectral vegetation indices to dead materials in mixed grasslands. *Remote Sens.* **2014**, *6*, 4289–4304. [CrossRef]
20. Jackson, R.D.; Huete, A.R. Interpreting vegetation indices. Interpreting vegetation indices. *Prev. Vet. Med.* **1991**, *11*, 185–200. [CrossRef]
21. Duan, M.; Gao, Q.; Wan, Y.; Li, Y.; Guo, Y.; Ganzhu, Z.; Liu, Y.; Qin, X. Biomass estimation of alpine grasslands under different grazing intensities using spectral vegetation indices. *Can. J. Remote Sens.* **2014**, *37*, 413–421. [CrossRef]
22. Numata, I.; Roberts, D.; Chadwick, O.; Schimel, J.; Galvao, L.; Soares, J. Evaluation of hyperspectral data for pasture estimate in the Brazilian Amazon using field and imaging spectrometers. *Remote Sens. Environ.* **2008**, *112*, 1569–1583. [CrossRef]
23. Biewer, S.; Fricke, T.; Wachendorf, M. Determination of dry matter yield from legume–grass swards by field spectroscopy. *Crop Sci.* **2009**, *49*, 1927–1936. [CrossRef]
24. Kumar, L.; Sinha, P.; Taylor, S.; Alqurashi, A.F. Review of the use of remote sensing for biomass estimation to support renewable energy generation. *J. Appl. Remote Sens* **2015**, *9*, 097696. [CrossRef]
25. Wrage, N.; Şahin Demirbağ, N.; Hofmann, M.; Isselstein, J. Vegetation height of patch more important for phytodiversity than that of paddock. *Agric. Ecosyst. Environ.* **2012**, *155*, 111–116. [CrossRef]
26. Scimone, M.; Rook, A.J.; Garel, J.P.; Sahin, N. Effects of livestock breed and grazing intensity on grazing systems: 3. Effects on diversity of vegetation. *Grass Forage Sci.* **2007**, *62*, 172–184. [CrossRef]
27. Jerrentrup, J.S.; Wrage-Mönnig, N.; Röver, K.-U.; Isselstein, J.; McKenzie, A. Grazing intensity affects insect diversity via sward structure and heterogeneity in a long-term experiment. *J. Appl. Ecol.* **2014**, *51*, 968–977. [CrossRef]
28. Pepperl; Fuchs. Sensing your needs: ENU Part No. 200237. 2010. Available online: http://www.pepperl-fuchs.us/usa/downloads_USA/Sensing-your-needs-2010-01-EN.pdf (accessed on 19 January 2017).
29. Klapp, E.; Stählin, A. Standorte, Pflanzengesellschaften und Leistung des Grünlandes. 122 Seiten mit 3 Karten und 20 Abbildungen. Verlag Eugen Ulmer, Stuttgart-S. 1936. *Z. Pflanzenernaehr. Dueng. Bodenk.* **1936**, *43*, 221–222.
30. R Development Core Team. *R: A Language and Environment for Statistical Computing*; R Foundation for Statistical Computing: Vienna, Austria, 2016.

31. Inoue, Y.; Penuelas, J.; Miyata, A.; Mano, M. Normalized difference spectral indices for estimating photosynthetic efficiency and capacity at a canopy scale derived from hyperspectral and CO_2 flux measurements in rice. *Remote Sens. Environ.* **2008**, *112*, 156–172. [CrossRef]
32. Rouse, J.W.; Haas, R.H.; Schell, J.A.; Deering, D.W. Monitoring vegetation systems in the Great Plains with ERTS. In *Third ERTS-1 Symposium*; Fraden, S.C., Marcanti, E.P., Becker, M.A., Eds.; Scientific and Technical Information Office, National Aeronautics and Space Administration: Washington, DC, USA, 1974; pp. 309–317.
33. Nelder, J.A. The statistics of linear models: back to basics. *Stat. Comput.* **1994**, *4*, 221–234. [CrossRef]
34. Nelder, J.A.; Lane, P.W. The computer analysis of factorial experiments: In memoriam—Frank Yates. *Am. Stat.* **1995**, *49*, 382–385. [CrossRef]
35. Diaconis, P.; Efron, B. Computer-intensive methods in statistics. *Sci. Am.* **1983**, *248*, 116–130. [CrossRef]
36. Biewer, S.; Fricke, T.; Wachendorf, M. Development of canopy reflectance models to predict forage quality of legume–grass mixtures. *Crop Sci.* **2009**, *49*, 1917. [CrossRef]
37. Marabel, M.; Alvarez-Taboada, F. Spectroscopic determination of aboveground biomass in grasslands using spectral transformations, support vector machine and partial least squares regression. *Sensors* **2013**, *13*, 10027–10051. [CrossRef] [PubMed]
38. Möckel, T.; Dalmayne, J.; Prentice, H.C.; Eklundh, L.; Purschke, O.; Schmidtlein, S.; Hall, K. Classification of grassland successional stages using airborne hyperspectral imagery. *Remote Sens.* **2014**, *6*, 7732–7761. [CrossRef]
39. Möckel, T.; Dalmayne, J.; Schmid, B.C.; Prentice, H.C.; Hall, K. Airborne hyperspectral data predict fine-scale plant species diversity in grazed dry grasslands. *Remote Sens.* **2016**, *8*, 133. [CrossRef]
40. Möckel, T.; Löfgren, O.; Prentice, H.C.; Eklundh, L.; Hall, K. Airborne hyperspectral data predict Ellenberg indicator values for nutrient and moisture availability in dry grazed grasslands within a local agricultural landscape. *Ecol. Indic.* **2016**, *66*, 503–516. [CrossRef]
41. Reddersen, B.; Fricke, T.; Wachendorf, M. A multi-sensor approach for predicting biomass of extensively managed grassland. *Comput. Electron. Agric.* **2014**, *109*, 247–260. [CrossRef]
42. Chen, P.; Haboudane, D.; Tremblay, N.; Wang, J.; Vigneault, P.; Li, B. New spectral indicator assessing the efficiency of crop nitrogen treatment in corn and wheat. *Remote Sens. Environ.* **2010**, *114*, 1987–1997. [CrossRef]
43. Anderson, M.; Neale, C.; LI, F.; Normann, J.; Kustas, W.; Jayanthi, H.; Chavez, J. Upscaling ground observations of vegetation water content, canopy height, and leaf area index during SMEX02 using aircraft and Landsat imagery. *Remote Sens. Environ.* **2004**, *92*, 447–464. [CrossRef]
44. Mutanga, O.; Skidmore, A.K. Narrow band vegetation indices overcome the saturation problem in biomass estimation. *Int. J. Remote Sens.* **2004**, *25*, 3999–4014. [CrossRef]
45. Psomas, A.; Kneubühler, M.; Huber, S.; Itten, K.; Zimmermann, N.E. Hyperspectral remote sensing for estimating aboveground biomass and for exploring species richness patterns of grassland habitats. *Int. J. Remote Sens.* **2011**, *32*, 9007–9031. [CrossRef]
46. Gherbin, P.; de Franchi, A.S.; Monteleone, M.; Rivelli, A.R. Adaptability and productivity of some warm-season pasture species in a Mediterranean environment. *Grass Forage Sci.* **2007**, *62*, 78–86. [CrossRef]